Published in final edited form as:
Scand J Immunol. 2008 July ; 68(1): 30–42. doi:10.1111/j.1365-3083.2008.02113.x.

Differential Effects of a Saturated and a Monounsaturated Fatty Acid on MHC Class I Antigen Presentation

S. R. Shaikh[*], **D. Mitchell**[†], **E. Carroll**[*], **M. Li**[‡], **J. Schneck**[‡], and **M. Edidin**[*]

[*] Department of Biology, Johns Hopkins University, Baltimore, MD

[†] Laboratory of Membrane Biochemistry and Biophysics, NIAAA/NIH, Bethesda, MD

[‡] Department of Pathology, Johns Hopkins University School of Medicine, Baltimore, MD, USA

Abstract

Lipid overload, associated with metabolic disorders, occurs when fatty acids accumulate in non-adipose tissues. Cells of these tissues use major histocompatibility complex (MHC) class I molecules to present antigen to T cells in order to eliminate pathogens. As obesity is associated with impaired immune responses, we tested the hypothesis that the early stages of lipid overload with saturated fatty acids (SFA) alters MHC class I antigen presentation. Antigen presenting cells (APC) were treated with either the saturated palmitic acid (PA), abundant in the high fat Western diet, or the monounsaturated oleic acid (OA), a component of the Mediterranean diet. PA-treatment lowered APC lysis by activated cytotoxic T lymphocytes and inhibited APC ability to stimulate naïve T cells. Inhibition of immune responses with PA was due to a significant reduction in MHC class I surface expression, inhibition in the rate of APC–T-cell conjugation, and lowering of plasma membrane F-actin levels. OA-treatment had no effect on antigen presentation and upon exposure with PA, prevented the phenotypic effects of PA. OA-treatment conferred protection against changes in antigen presentation by accumulating fatty acids into triglyceride-rich lipid droplets of APC. Our findings establish for the first time a link between the early stages of lipid overload and antigen presentation and suggest that dietary SFA could impair immunity by affecting MHC I-mediated antigen presentation; this could be prevented, paradoxically, by accumulation of triglycerides rich in monounsaturated fatty acids.

Introduction

Obesity is now regarded as an epidemic on a worldwide scale, a consequence of nutritional and genetic factors [1–3]. High fat diets are major factors that promote the development of obesity, which results in disorders including cardiovascular disease, hypertension, diabetes mellitus and immune dysfunction with increased susceptibility to infection [3]. One major factor that predisposes obese individuals to infection is nutritional status [4]. Saturated fatty acids (SFA) in particular are abundant in the ‘high fat Western diet’ and could contribute to immunosuppression [5–8]. As an example, recent studies show that viral disease progression

Correspondence to: Dr S. R. Shaikh, Department of Biology, Johns Hopkins University, 3400 North Charles Street, Mudd Hall Room 45, Baltimore, MD 21218, USA. saameshaikh@gmail.com.

Contributions

Saame Raza Shaikh – designed experiments, conducted experiments, analysed data, wrote manuscript; Drake Mitchell – designed and conducted fluorescence anisotropy measurements and analysed data, Elizabeth Carroll – conducted cell viability experiments; Matt Li – conducted mixed lymphocyte reactions for all studies and some spleen isolations; Jonathan Schneck – designed experiments, contributed to data analysis, Michael Edidin – designed experiments, contributed to data analysis, revised and edited manuscript.

in animals fed high fat diets, enriched in SFA, is accelerated, compared to control animals on a normal diet [8,9].

It is known that high fat diets, enriched with SFA, can impair immune responses by affecting inflammatory pathways through the adipokine, cytokine and chemokine networks [9–12]. Very little is known about the direct effects of SFA on antigen recognition at any stage of an immune response. A few studies do show that dyslipidemia, through either dietary or genetic manipulations, impairs the ability of antigen presenting cells (APC) to stimulate naïve T cells [7,13–15]. For instance, diet-induced dyslipidemia in C57/BL6 mice impaired activation of CD8α^- dendritic cells (DC) and consequently, host resistance to *Leishmani major* infection was compromised [13]. Similarly, another study showed that APC isolated from DO10.11 mice fed high-fat diets, rich in SFA, poorly stimulated naïve T cells from mice fed normal diets [7]. The molecular mechanisms by which SFA affect the cell biology of antigen presentation have not been investigated.

In the present study, we tested the effects of the early stages of lipid overload with palmitic acid (PA) and oleic acid (OA) on major histocompatibility complex (MHC) class I-mediated antigen presentation. Lipid overload, associated with metabolic disorders including obesity, is the accumulation of fatty acids in non-adipose tissues [16]. Tissue cells use MHC class I molecules, carrying antigenic peptides, to trigger responses from cytotoxic T lymphocytes in order to eliminate pathogens [17]. We compared the effects of PA, abundant in the high fat Western diet, to OA, a monounsaturated fatty acid (MUFA), which is an abundant plasma fatty acid and a component of the Mediterranean diet [18]. MUFA are hypothesized to be beneficial for prevention of obesity and other metabolic diseases and for immune function [19,20]. Our findings show that PA and OA have differential effects on antigen presentation, which correlated with their metabolic fates. PA, but not OA, downregulated APC function above a concentration of 250 μM and OA prevented this. Our earlier work showed that a lower concentration of 100 μM PA had no effect on antigen presentation [21]. This study establishes a new link between the early stages of lipid overload, immune responses and triglyceride accumulation.

Materials and methods

Cells

Human T2 cells are transporter associated with antigen processing (TAP)-deficient and express K^b, the mouse MHC class I allele. T2-K^b APC were grown in RPMI-1640 1X supplemented with 10% FBS and 5% glutamine. T2 cells stably transfected with a K^b-YFP construct also contained 300 μg/ml G418 for plasmid selection in the medium. Cells were cultured at 37 °C in a 95% O_2/5% CO_2 atmosphere.

Fatty acid treatment of APC

T2-K^b cells were incubated for 12 h at 37 °C with free fatty acids (FFA). PA (Sigma Chemical Co., St Louis, MO, USA) and OA (Nu Check Prep, Elysian, MN, USA) were delivered as complexes of FFA/BSA (6.5:1) (fatty acid-free BSA; Roche Biochemicals, Indianapolis, IN, USA) as described previously [21]. The ratio of FFA/BSA reflects *in vivo* levels of hyperlipidemia [22]. FFA/BSA complexes were added from 10 mM stocks to RPMI-1640 1X medium with 5% FBS and 5% glutamine. 1×10^6 cells were cultured in 6-well plates at a concentration of 1×10^5/ml. All preparations of OA-containing lipids were made under a gentle stream of nitrogen gas in low light conditions using degassed reagents to prevent oxidation. Fresh FFA/BSA stocks were utilized for all experiments in order to prevent the formation of micelles. Cell viability was confirmed with trypan blue exclusion and 7-amino-actinomycin D (7-AAD) staining. Uptake of fatty acids was confirmed with gas chromatography.

Annexin V staining

Flow cytometry was used to assess apoptosis and to measure CTL lysis of APC. Apoptosis measurements with Annexin V-Cy5 and 7-AAD were performed according to the manufacturer's protocol (BD Biosciences Pharmingen, San Diego, CA, USA). Early apoptotic cells were identified as Annexin V-Cy5$^+$7-AAD$^-$ and late apoptotic cells were Annexin V-Cy5$^+$7-AAD$^+$. The apoptotic index (AI) was calculated as: $AI = [A_{FFA} - A_{BSA}]/[100 - A_{BSA}] \times 100$, where A_{FFA} is the percentage of cells that were apoptotic upon lipid treatment and A_{BSA} is the percentage of cells that were apoptotic in the control BSA condition [23]. Fatty acid treatment did not affect cell viability (>85%) at 12 h of treatment as assessed by Annexin V staining (Fig. S1). These measurements show that the cells are in the early stages of lipid overload prior to becoming lipotoxic (Fig. S1).

Peptide loading of APC

Peptides can be loaded directly onto MHC class I molecules of T2-K^b cells [24]. After lipid treatment at 37 °C, cells were transferred from 6-well plates to 15 ml Falcon tubes, incubated at room temperature for 5 h in the BSA or fatty acid containing medium followed by a 1 nM SIY (SIYRYYGL) peptide pulse for 1 h at 37 °C in serum-free medium [25]. After peptide loading, cells were extensively washed with normal medium to ensure removal of excess peptide, prior to use for experimentation. Peptide loading was confirmed by flow cytometry measurements of surface MHC class I.

Purification of naïve CD8$^+$ T cells

Naïve T cells were isolated from spleens of 2C transgenic mice with a CD8 negative selection kit (R & D Systems, Minneapolis, MN, USA) using the manufacturer's protocol. Briefly, splenocytes ($\leq 10^8$ cells), resuspended into 1X column buffer, were mixed with monoclonal antibody cocktail binding B cells, monocytes and non-CD8$^+$ T cells. After 15 min of incubation, the cells were washed twice in 1X column buffer, resuspended into 2 ml of buffer, and loaded onto a washed CD8 subset column to incubate at room temperature for 10 min. The column was then eluted with 10 ml of 1X column buffer. Cells were cultured in RMPI-1640 1X medium supplemented with 10% FBS and 5% glutamine.

Activation of naïve T cells

Naïve CD8$^+$ T cells from the spleens of 2C transgenic mice were activated using a mixed lymphocyte reaction. Splenocytes isolated from the spleens of BALB/*c* mice were gamma irradiated (3000 rads) and mixed with naïve T cells at a 1.75/1.25 ratio in 24-well plates at 2×10^6 cells/ml. Cells were grown in complete RMPI medium supplemented with IL-2 (10 U/ml) (Roche Biochemicals).

Effector T-cell lysis assays of target APC

Target T2-K^b cells were lipid modified as described above, pelleted, and incubated with 100 μCi ^{51}Cr (Perkin Elmer, Boston, MA, USA) for 1 h in serum-free medium followed by three washes to remove excess ^{51}Cr. Effector (activated CTL from 2C transgenic mice) and target cells were then cultured in 96-well plates at differing ratios for 4 h at 37 °C in a final volume of 200 μl. Cells were pelleted and 100 μl of the supernatant was assayed for activity with a gamma counter. Maximal ^{51}Cr release was induced by the addition of 1 M HCl. Percent specific lysis (SL) was calculated with the following relation: %SL = (sample cpm − spontaneous cpm)/(maximal release cpm − spontaneous release cpm) × 100. Lysis of target APC with 2C CTL was also determined using Annexin V-Cy5, 7-AAD staining as described above. For these measurements, effector and target cells were only cultured at 37 °C for 2 h at an effector to target ratio of 5.

Naïve T-cell stimulation assay

Control or fatty acid-modified T2-K^b cells, pulsed with SIY peptide, were washed in normal RPMI medium and subsequently mixed with naive $CD8^+$ T lymphocytes at a ratio of 1/1. On average, 200,000 cells were used for each cell type. Activation was measured with flow cytometry 6 h later using anti-CD8a-PE and anti-CD69-PECy7 (BD Pharmingen) staining.

Flow cytometry

Measurements were made on a FACSCalibur flow cytometer (Becton Dickinson, San Jose, CA, USA) equipped with a 488 nm argon laser and a 647 nm diode laser. For all experiments, cell numbers between different samples were equalized to at least 2×10^5 cells/sample. Samples were washed in phosphate-buffered saline (PBS) twice, stained with saturating levels of fluorescent antibody (for MHC I studies) for 30 min on ice, followed by two additional washes in PBS. Data were acquired on a minimum of 1×10^4 gated live cells. Dead cells were stained with 7-AAD or propidium iodide.

MHC class I surface expression studies

For studies of MHC class I expression, we utilized the monoclonal antibody 20.8.4s (anti-monomorphic epitope) conjugated to Cy5, which recognized K^b loaded with peptide. The antibody was purified from hybridoma supernatants using Protein-A affinity chromatography. 20.8.4s was conjugated to Cy5 dye using a standard kit (Amersham Biosciences, Piscataway, NJ, USA). For flow cytometry surface expression studies, cell samples not expected to bind a given primary antibody were used as controls. An additional control was the use of excess unlabelled antibody to block binding of fluorescently labelled antibody. For all experiments, background auto-fluorescence was established with unstained cells.

Conjugation assay

Conjugation experiments were conducted as previously described [21]. Briefly, CTL were loaded with 1,1′-dioctadecyl-3,3,3′,3′-tetramethylindodicarbocyanine perchlorate, DiD, (Invitrogen, Carlsbad, CA, USA) for 1 h in Hanks' Balanced Salt Solution (HBSS) (Mediatech Inc., Herndon, VA, USA) at 37 °C and then mixed at a 1:1 ratio with control or lipid modified T2 cells stably transfected with K^b-YFP. Cells were incubated at 37 °C for 15 min and conjugate formation was inhibited by adding cold Hanks Balanced Salt Solution and placing the samples on ice. Formation of conjugates, which were double positive for DiD and YFP, was determined with flow cytometry.

Confocal fluorescence microscopy

The metabolic fate of fatty acids in response to lipid feeding in T2-K^b cells was assessed using confocal fluorescence microscopy. T2-K^b cells were treated with fatty acids in the presence of 4.0 μg/ml C_1,C_{12} BODIPY (Invitrogen) for 12 h in RPMI medium supplemented with 5% FBS and glutamine in the absence of phenol red (Mediatech Inc.). Cells were then washed twice in PBS. Fatty acid treated APC were stained with 1.0 μg/ml C_{16}BODIPY for 25 min or 2.5 μg/ml Nile Red (Invitrogen) for 1 h followed by two washes in PBS. Cells were fixed in 4% paraformaldehyde, washed twice in PBS and stained with 1.0 μg/ml DAPI (Invitrogen) for 15 min followed by two washes in PBS. For assessment of changes in F-actin levels, cells were permeabilized for 10 min in 0.1% Triton X-100 and then treated with 2 μM phalloidin (Invitrogen) for 25 min. Cells were subsequently washed with PBS twice. For all microscopy measurements, cells were placed in capillary tubes (Vitrotubes, Mt. Lks, NJ, USA) and mounted on slides. Fluorescence images were collected using a confocal microscope (Zeiss LSM 510 META, Carl Zeiss MicroImaging, Thornwood, NY, USA). Gain and pinhole settings were kept constant between different samples within an experiment.

Radiolabel release

T2-K^b cells were treated as described above and spiked with 10 μCi [^{3}H]PA (specific activity 31 Ci/mmol) or [^{3}H]OA (specific activity 33.4 Ci/mmol) (Perkin Elmer). A total of 100,000 cells were placed in a final volume of 200 μl of normal medium in 96-well plates. At differing time points, cells were pelleted and supernatant and pellet fractions were counted for radioactivity using a scintillation counter.

Time-resolved fluorescence anisotropy

1×10^6 T2-K^b cells were washed in HBSS and diluted to 0.25×10^6/ml HBSS. DPH (Invitrogen, Eugene, OR, USA) was added to the cells at a lipid to probe ratio of 300:1 and incubated at 37 °C for 30 min. DPH fluorescence lifetime and differential polarization were measured using an ISS K2 multifrequency cross-correlation phase spectrofluorimeter (ISS, Urbana, IL, USA). Excitation at 351 nm was provided by an Innova 307 argon ion laser (Coherent, Santa Clara, CA, USA). Lifetime and differential polarization data were acquired at 37 °C at 15 modulation frequencies, logarithmically spaced from 5 to 150 MHz. Total fluorescence intensity decays were analysed with the sum of three exponential decays. Reported values are the intensity-weighted average, $<\tau>$, of the resulting three exponential time constants. Anisotropy decays were analysed using the Brownian rotational diffusion (BRD) model and the results were interpreted in terms of an angular distribution function of DPH, $f(\theta)$, which is symmetric about the membrane normal [26]. Relative acyl chain packing was quantified using the disorder parameter, F_{random}, which is proportional to the overlap of the DPH orientational probability distribution, $f(\theta)\sin\theta$, with randomly oriented DPH. The BRD model quantifies probe motion in terms of the diffusion coefficient for DPH rotation about its long axis (perpendicular), D_{perp}. Fluorescence anisotropy decays were also analysed using an empirical sum-of-three-exponentials model. In this analysis, probe orientational order is summarized by the order parameter S, where $S = (r_\infty/r_o)^{1/2}$, and uncorrelated rotational motion is characterized by the three rotational time constants, ϕ_i. The three rotational time constants and their associated pre-exponential factors were used to calculate the weighted average rotational correlation time, $<\phi>$.

Analysis

Data were plotted in ORIGIN (7.0; OriginLab Corporation, Northampton, MA, USA) or GRAPHPAD PRISM (4.0; Graph-Pad Software, San Diego, CA, USA). Flow cytometry data were analysed with CELL QUEST software (Becton Dickinson, San Jose, CA, USA). Fluorescence images were analysed using IMAGE J Software (NIH, available at http://rsb.info.nih.gov.ij). All analyses of time-resolved differential polarization data were performed with NONLIN, with subroutines specifying the fitting functions written by the authors (DCM). Statistical significance was establshed against a common control (BSA) by performing a one-way ANOVA followed by a Dunnett's *t*-test. *P*-values <0.05 were considered significant. For fluorescence microscopy studies, statistical signficance was established using statistical box plots. Differences in the horizontal displacement of notches between box plots indicate statistical signficance [27].

Results

APC treated with PA are resistant to lysis by activated CTL

We compared the effects of BSA-, PA-, and OA-treatment for 12 h on lysis of T2-K^b cells by activated $CD8^+$ CTL from the 2C TcR transgenic mouse using ^{51}Cr release (Fig. 1A) and Annexin V-Cy5 binding (Fig. 1B), as measures of target cell death. PA-treated cells were lysed significantly less than BSA-treated cells. The effects of PA on lysis were dose-dependent (Fig. 1C) and time-dependent (data not shown). Cells treated with 250 μM PA showed ~20%

inhibition in lysis and maximal inhibition was ~35% with 500 μM PA. No significant effects on lysis were observed with OA-treatment.

PA-treated APC are not efficient activators of naïve T cells

We tested the ability of T2-K^b cells, treated with BSA, PA, or OA for 12 h, to activate naïve 2C $CD8^+$ T cells. Early T-cell activation was measured by assessing the percentage of $CD8^+$ T cells that upregulated $CD69^+$, an early marker of activation (Fig. 2A). Approximately 64% of the T cells activated with BSA-treated control APC were $CD8^+$ $CD69^+$ (Fig. 2B). Treatment with 500 μM PA significantly lowered the percentage of $CD8^+$ $CD69^+$ cells to ~45%. T2-K^b cells treated with 500 μM OA activated ~70% of the T cells, similar to the effects with BSA control cells. We also assessed the degree of T-cell activation by analysing the level of CD69 expression of the $CD8^+$ $CD69^+$ T-cell population. T cells had significantly less CD69 surface expression after activation by T2-K^b cells treated with 500 μM PA, corresponding to a ~20–25% change relative to the BSA control (Fig. 2C). No significant effect was observed with OA.

Effects of PA and OA are independent of free-fatty acid release

We investigated the mechanisms by which PA-treatment of APC lowered CTL lysis relative to controls. It has been reported that nanomolar levels of unbound free fatty acids in the medium can inhibit CTL killing of target cells by affecting the CTL rather than the target [28–30]. We tested this potential mechanism by assessing the amount of released radiolabelled fatty acids from the APC. T2-K^b cells were treated with 500 μM PA or OA spiked respectively with [^{3}H] PA or [^{3}H]OA for 12 h at 37 °C. We then measured the amount of radiolabel released in the supernatant and cell pellets over 120 min, in the absence of T cells (Fig. S2). The majority of the radiolabels remained in the cell pellets, with no significant change over the time course. Less than 10% of the total radioactivity from the labelled fatty acids was in the supernatants for each time point. This may be an overestimate since labelled fatty acids may also include neutral and polar lipids shed from the plasma membrane. In any event, our data argue against release of free fatty acids as a mechanism by which PA-treated APC are resistant to CTL lysis.

PA-treated APC have lower MHC class I surface levels than controls

We further explored mechanisms by which PA-treatment would affect antigen presentation by APC to activated 2C CTL. Relative to the BSA control, PA-treatment at 250–500 μM lowered MHC class I levels. Maximal median fluorescence intensities were lowered from ~125 for BSA-treated cells to ~55 (Fig. 3A) with 500 μM PA, corresponding to a ~65% change (Fig. 3B). We also found that 500 μM OA lowered MHC class I levels by ~30%. The reduction in MHC class I surface levels with PA was not sufficient to completely account for the reduction in lysis by CTL based on previous calibration measurements [21].

PA-treatment of APC inhibits the rate of APC–CTL conjugation

Another mechanism by which PA-treatment could downregulate APC function is a change in conjugation with CTL. We tested the effects of BSA-, PA-, and OA-treatment on T2-K^b-YFP conjugation to DiD loaded CTL. Conjugates were identified by flow cytometry as YFP^+ DiD^+ (Fig. 4A). PA-treatment inhibited the rate of APC–CTL conjugation (Fig. 4B). We tested for dose-dependent effects of PA on conjugation at 15 min. Indeed, PA-treatment at 250 and 500 μM inhibited conjugation respectively by 50 and 70% (Fig. 4C). This level of dose-dependent change was sufficient to account for the functional effects of PA (Fig. 1). OA-treatment had no significant effect on APC–T-cell conjugation.

Concomitant OA-treatment blocks the effects of PA on antigen presentation

As OA-treatment of cells did not inhibit antigen presentation to T cells, we tested if co-supplementation of OA and PA could rescue the effects of PA on antigen presentation. We first verified that treatment of T2-K^b cells for 12 h at 37 °C with 500 μM OA added to 500 μM PA did not affect cell viability (Fig. 5A). We tested CTL lysis of T2-K^b cells treated with 500 μM PA + 500 μM OA at an E/T = 5. Indeed, the percentage of PA + OA-treated cells that were undergoing apoptosis, as measured by Annexin V-Cy5 (Fig. 5B), was nearly identical to the BSA- and OA-treated cells (Fig. 5C). Thus, OA-treatment has a protective effect on antigen presentation in the presence of PA. OA did not act by blocking uptake of PA into the cell with radiolabelled fatty acid uptake experiments (data not shown).

OA sequesters PA into triglyceride-rich lipid droplets

We speculated that the metabolic fate of OA-treatment was related to its lack of functional effect on antigen presentation. APC were treated with BSA, 500 μM PA, 500 μM OA, and 500 μM PA + 500 μM OA and spiked with C_1C_{12}BODIPY for 12 h. The majority of the fluorescence signal was localized to the ER membrane irrespective of fatty acid treatment (Fig. 6A). Lipid overload with OA resulted in the formation of large pools of fatty acids. Addition of OA to PA-treated cells also appeared to divert the probe into lipid pools (Fig. 6A). We speculated that these pools represented lipid droplets, which we verified with Nile Red staining (Fig. 6A). Indeed, T2-K^bs showed a greater number of lipid droplets in the OA and PA + OA-treated cells compared to BSA- or PA-treated cells (Fig. 6A). We then verified that PA in the presence of OA was sequestered into lipid droplets by staining with C_{16}BODIPY. We quantified the area occupied by the C_1C_{12}BODIPY, Nile Red, or C_{16}BODIPY probes in lipid droplets by measuring the area occupied by the probe in square pixels per cell (Fig. 6B). Statistical box plots show that treatment of APC with OA resulted in increased uptake of fatty acids into lipid droplets (Fig. 6B). We verified our microscopy results with Nile Red by using flow cytometry (data not shown), the data were consistent with the microscopy measurements.

PA and OA have differential effects on plasma membrane structure

It has been shown that inhibition in antigen presentation is linked to changes in plasma membrane structure [31]. We tested the effects of fatty acid treatment on lipid and submembrane cytoskeleton regions of the plasma membrane. Changes in lipid order and dynamics were assessed using fluorescence lifetime and dynamic anisotropy measurements of the fluorescent membrane probe DPH. Figure 7A,B summarize the results of analysing the DPH anisotropy decays in terms of an empirical sum-of-three exponentials model. 500 μM OA and 500 μM PA + 500 μM OA decreased the order parameter for DPH, S, by 40–50% (Fig. 7A). A slight increase in order was measured following 500 μM PA-treatment, but this did not reach statistical significance. The rotational correlation time was increased with all three lipid-treatment conditions with an acceleration of DPH motion by 25–40% (Fig. 7B). Similar effects of all fatty acid treatments also were reported by the BRD model analysis (Table 1). Qualitatively identical results were obtained for both DPH orientational order and DPH rotational motion. The increase in fluorescence lifetime with all the fatty acid treatments (Table 1) implies decreased water penetration into the bilayer region [26], suggesting some changes in the headgroup region of the plasma membrane.

As changes in acyl chain packing and headgroup order did not correlate with a change in conjugation of APC to activated 2C CTL, we tested for the effects of fatty acid treatment on the actin cytoskeleton. Using confocal fluorescence microscopy, we measured phalloidin binding to F-actin on APC treated with BSA, 500 μM PA, 500 μM OA and 500 μM PA + 500 μM OA (Fig. 7C). Quantitative image analysis of phalloidin intensity levels showed that treatment of APC with PA lowered the total levels of F-actin by ~50% (Fig. 7D). No changes in F-actin were observed after OA- or PA + OA-treatment.

Discussion

This is the first study to model the early stages of lipid overload in antigen presenting cells. Lipid overload, associated with a number of metabolic disorders, occurs when adipose tissue is unable to handle excess fat and a spillover occurs into other tissues (e.g. skeletal, cardiac, kidney, liver, pancreas, etc) [16,32]. All nucleated cells have MHC class I molecules and can present antigen to cognate CTL for the elimination of intracellular pathogens. We therefore tested the effects of lipid overload with PA and OA on MHC class I-mediated antigen presentation. Our data show PA, but not OA, inhibits antigen presentation to CTL (Fig. 1), this may be one mechanism by which individuals with lipid overload with saturated fatty acids are immunocompromised. In addition, our data on stimulation of naïve T cells (Fig. 2) also suggest the lipid overload with PA could affect B-cell activation of naïve T cells [33]. This is in agreement with reports on dyslipidemia impairing DC activation of naïve T cells [7,15].

We have ruled out the possibility of free fatty acid release as a mechanism by which APC function is affected (Fig. S2). Our mechanistic findings are consistent with other studies that have shown that changes in lipid and/or cytoskeleton organization have an important effect on antigen presentation. Infection of APC with *Leishmania donovani* resulted in disruption of 'lipid raft' microdomains which lowered antigen presentation by macrophages to T cells [34]. Our laboratory has shown that cholesterol depletion from APC can enhance antigen presentation to CTL by increasing MHC class I clustering [25,35]. MHC I clustering was increased due to a reduction in the levels of the signaling lipid phosphatidylinositol 4,5-bisphosphate (PIP2), which altered the organization of the actin cytoskeleton [35]. Others have shown that de-clustering of MHC I molecules in B lymphoblast APC increased resistance of APC to CTL lysis [36]. Finally, some tumour cells evade CTL lysis by modifying target cell actin levels [37]. In the present study, we found that PA-treatment of APC inhibited conjugation to CTL which correlated with a change in F-actin levels (Fig. 7). Future studies will examine the role of palmitic acid in the formation of the immunological synapse, which is actin dependent [38].

Differential cellular uptake of PA and OA may affect the underlying functional response to lysis by activated CTL. PA-treatment does not affect acyl chain order (Fig. 7A,B) but does result in greater modification of plasma membrane F-actin (Fig. 7C,D). We speculate that PA exerts its effects on the actin cytoskeleton through a combination of physical, metabolic, or genetic changes, which are not mutually exclusive. PA may be creating local membrane defects in the plasma membrane, which could then uncouple the actin cytoskeleton to the inner leaflet of the plasma membrane. This possibility would be consistent with a recent molecular dynamics simulation study that proposed that palmitate incorporation into the membrane could create membrane defects [39]. This would also be consistent with our anisotropy measurements (Fig. 7A,B) (Table 1).

The effects of PA on the actin cytoskeleton may also be linked to its metabolic fate. It is well established that palmitate serves as an extrinsic stimuli for inducing apoptosis [40]. Although the APC are not apoptotic with PA-treatment at 12 h (Fig. S1), it is entirely plausible that PA may be increasing the initial mediators of apoptosis (e.g. ceramides, ROS), which could modify the actin cytoskeleton [41]. The metabolic argument is supported by data to show that sequestering PA into lipid droplets with OA can prevent the effects on antigen presentation (Figs. 5 and 6), consistent with a role for MUFA in preventing apoptosis [32]. Finally, PA-treatment may induce changes at the gene level. A recent study showed that select tumour cells evade CTL lysis by lowering target cell F-actin levels, which was related to overexpression of actin-related genes, *ephrin-A2* and *scinderin*, which also have a role in apoptosis [37]. Perhaps, PA exerts its effects on actin by affecting the expression of genes involved in actin remodelling. Future studies will test how PA-treatment could affect the formation of the immunological

synapse by modifying cytoskeleton proteins besides F-actin and membrane lipid/protein lateral organization and if these changes are related to alterations in the expression of actin-related genes.

Finally, a striking features of this study is that the mechanisms by which SFA exert their effects are highly similar to the way in which n-3 PUFA, which are well known immunosuppressants, downregulate MHC class I-and class II-mediated antigen presentation [21,42–45]. We previously showed that treatment of human B lymphoblasts with either n-3 or n-6 PUFA increased their resistance to alloreactive T-cell lysis by inhibiting MHC class I ER to Golgi trafficking and APC–T-cell conjugation [21]. It is important to note that in our previous study, we observed no effect of 100 μM PA-treatment on antigen presentation; however, we did not test higher concentrations of PA, as used in this study [21]. A number of laboratories have shown that PUFA inhibited MHC class II antigen presentation, which correlated with changes in MHC class II and adhesion molecule surface expression [42,43,46]. The Stulnig laboratory has also shown that treatment of T cells with PUFA inhibits the formation of an immunological synapse by blocking cytoskeleton organization [47]. We propose that SFA, modelling conditions of hyperlipidemia and PUFA, modelling intake of fish oils, could downregulate immune responses using similar mechanisms. However, more experiments with a wide range of SFA and PUFA will be required to assess if these fatty acids have similar effects on antigen presentation through MHC class I and II.

Summary

In summary, our studies show that PA-treatment of APC downregulates antigen presentation to cognate T cells which is driven in part by changes in MHC class I surface expression, APC–T-cell conjugation, and modification of F-actin levels. OA-treatment has no effect on antigen presentation and can prevent the effects of PA. The mechanisms of downregulation are highly similar to those observed with polyunsaturated fatty acids on MHC class I and II-mediated antigen presentation. Downregulation of antigen presentation with SFA induced lipid overload may be a potential mechanism by which high fat diets enriched in SFA render obese individuals to be immunocompromised. Current studies are underway in animals to assess lipid overload in immune cells and potential immunosuppression with high fat diets through the MHC class I pathway.

Supplementary Material

Refer to Web version on PubMed Central for supplementary material.

Acknowledgments

We thank the members of the Schneck laboratory for obtaining 2C transgenic mice during the course of this study and Dr Maya Everett for useful discussions. This research was supported by grants from the NIH to M.E. (AI14584) and J.S. (AI29575 and AI24129). S.R.S. was supported from a training grant to M. Soloski (5T32-AI07). The authors have no financial conflicts of interest.

References

1. Lamas O, Marit A, Wyatt H. Obesity and immunocompetence. Eur J Clin Nutr 2002;56 (Suppl 3):S42–5. [PubMed: 12142961]
2. Hill JO, Melanson EL, Wyatt HT. Dietary fat intake and regulation of energy balance: implications for obesity. J Nutr 2000;130:284–8.
3. Bray GA, Popkin BM. Dietary fat intake does affect obesity! Am J Clin Nutr 1998;68:1157–73. [PubMed: 9846842]

4. Falagas ME, Kompoti M. Obesity and infection. Lancet Infect Dis 2006;6:438–46. [PubMed: 16790384]
5. Marcos A, Nova E, Montero A. Changes in the immune system are conditioned by nutrition. Eur J Clin Nutr 2003;57 (Suppl 1):S66–9. [PubMed: 12947457]
6. Lissner L, Heitmann BL. Dietary fat and obesity: evidence from epidemiology. Eur J Clin Nutr 1995;49:79–90. [PubMed: 7743988]
7. Verwaerde C, Delanoye A, Macia L, Tailleux A, Wolowczuk I. Influence of high-fat feeding on both naive and antigen-experienced T-cell immune response in DO10.11 mice. Scand J Immunol 2006;64:457–66. [PubMed: 17032237]
8. Mansfield KG, Carville A, Wachtman L, et al. A diet high in saturated fat and cholesterol accelerates simian immunodeficiency virus disease progression. J Infect Dis 2007;196:1202–10. [PubMed: 17955439]
9. Smith AG, Sheridan PA, Harp JB, Beck MA. Diet-induced obese mice have increased mortality and altered immune responses when infected with influenza virus. J Nutr 2007;137:1236–43. [PubMed: 17449587]
10. Golay A, Bobbioni E. The role of dietary fat in obesity. Int J Obes Relat Metab Disord 1997;21 (Suppl 3):S2–11. [PubMed: 9225171]
11. de Wilde J, Mohren R, van den Berg S, et al. Short-term high fat-feeding results in morphological and metabolic adaptations in the skeletal muscle of C57BL/6J mice. Physiol Genomics 2008;32:360–9. [PubMed: 18042831]
12. Miyazaki Y, Iwabuchi K, Iwata D, et al. Effect of high fat diet on NKT cell function and NKT cell-mediated regulation of Th1 responses. Scand J Immunol 2008;67:230–7. [PubMed: 18226013]
13. Shamshiev AT, Ampenberger F, Ernst B, Rohrer L, Marsland BJ, Kopf M. Dyslipidemia inhibits toll-like receptor-induced activation of CD8alpha-negative dendritic cells and protective Th1 type immunity. J Exp Med 2007;204:441–52. [PubMed: 17296788]
14. Angeli V, Llodra J, Rong JX, et al. Dyslipidemia associated with atherosclerotic disease systemically alters dendritic cell mobilization. Immunity 2004;21:561–74. [PubMed: 15485633]
15. Macia L, Delacre M, Abboud G, et al. Impairment of dendritic cell functionality and steady-state number in obese mice. J Immunol 2006;177:5997–6006. [PubMed: 17056524]
16. Unger RH. Lipid overload and overflow: metabolic trauma and the metabolic syndrome. Trends Endocrinol Metab 2003;14:398–403. [PubMed: 14580758]
17. Janeway, CA. Immunobiology. Vol. 6. New York: Garland Science Publishing; 2005.
18. Yaqoob P. Monounsaturated fatty acids and immune function. Eur J Clin Nutr 2002;56 (Suppl 3):S9–13. [PubMed: 12142954]
19. Wahle KW, Caruso D, Ochoa JJ, Quiles JL. Olive oil and modulation of cell signaling in disease prevention. Lipids 2004;39:1223–31. [PubMed: 15736919]
20. Paniagua JA, Gallego de la Sacristana A, Romero I, et al. Monounsaturated fat-rich diet prevents central body fat distribution and decreases postprandial adiponectin expression induced by a carbohydrate-rich diet in insulin-resistant subjects. Diabetes Care 2007;30:1717–23. [PubMed: 17384344]
21. Shaikh SR, Edidin M. Immunosuppressive effects of polyunsaturated fatty acids on antigen presentation by human leukocyte antigen class I molecules. J Lipid Res 2007;48:127–38. [PubMed: 17074926]
22. Kleinfeld AM, Prothro D, Brown DL, Davis RC, Richieri GV, DeMaria A. Increases in serum unbound free fatty acid levels following coronary angioplasty. Am J Cardiol 1996;78:1350–4. [PubMed: 8970405]
23. Cnop M, Hannaert JC, Hoorens A, Eizirik DL, Pipeleers DG. Inverse relationship between cytotoxicity of free fatty acids in pancreatic islet cells and cellular triglyceride accumulation. Diabetes 2001;50:1771–7. [PubMed: 11473037]
24. Sykulev Y, Brunmark A, Tsomides TJ, et al. High-affinity reactions between antigen-specific T-cell receptors and peptides associated with allogeneic and syngeneic major histocompatibility complex class I proteins. Proc Natl Acad Sci U S A 1994;91:11487–91. [PubMed: 7972089]
25. Fooksman DR, Gronvall GK, Tang Q, Edidin M. Clustering class I MHC modulates sensitivity of T cell recognition. J Immunol 2006;176:6673–80. [PubMed: 16709826]

26. Mitchell DC, Litman BJ. Molecular order and dynamics in bilayers consisting of highly polyunsaturated phospholipids. Biophys J 1998;74:879–91. [PubMed: 9533699]
27. McGill R, Tukey JW, Larsen WA. Variations of box plots. Am Stat 1978;32:12–6.
28. Kleinfeld AM, Okada C. Free fatty acid release from human breast cancer tissue inhibits cytotoxic T-lymphocyte-mediated killing. J Lipid Res 2005;46:1983–90. [PubMed: 15961785]
29. Richieri GV, Kleinfeld AM. Free fatty acids inhibit cytotoxic T lymphocyte-mediated lysis of allogeneic target cells. J Immunol 1990;145:1074–7. [PubMed: 2380550]
30. Richieri GV, Kleinfeld AM. Free fatty acid perturbation of transmembrane signaling in cytotoxic T lymphocytes. J Immunol 1989;143:2302–10. [PubMed: 2789260]
31. Dahl JS, Dahl CE, Levine RP. Role of lipid fatty acyl composition and membrane fluidity in the resistance of acholeplasma laidlawii to complement-mediated killing. J Immunol 1979;123:104–8. [PubMed: 448140]
32. Listenberger LL, Han X, Lewis SE, et al. Triglyceride accumulation protects against fatty acid-induced lipotoxicity. Proc Natl Acad Sci U S A 2003;100:3077–82. [PubMed: 12629214]
33. Pape KA, Catron DM, Itano AA, Jenkins MK. The humoral immune response is initiated in lymph nodes by B cells that acquire soluble antigen directly in the follicles. Immunity 2007;26:491–502. [PubMed: 17379546]
34. Chakraborty D, Banerjee S, Sen A, Banerjee KK, Das P, Roy S. Leishmania donovani affects antigen presentation of macrophage by disrupting lipid rafts. J Immunol 2005;175:3214–24. [PubMed: 16116212]
35. Kwik J, Boyle S, Fooksman D, Margolis L, Sheetz MP, Edidin M. Membrane cholesterol, lateral mobility, and the phosphatidylinositol 4,5-bisphosphate-dependent organization of cell actin. Proc Natl Acad Sci U S A 2003;100:13964–9. [PubMed: 14612561]
36. Bodnar A, Bacso Z, Jenei A, et al. Class I HLA oligomerization at the surface of B cells is controlled by exogenous beta(2)-microglobulin: Implications in activation of cytotoxic T lymphocytes. Int Immunol 2003;15:331–9. [PubMed: 12618477]
37. Abouzahr S, Bismuth G, Gaudin C, et al. Identification of target actin content and polymerization status as a mechanism of tumor resistance after cytolytic T lymphocyte pressure. Proc Natl Acad Sci U S A 2006;103:1428–33. [PubMed: 16432193]
38. Dustin ML, Cooper JA. The immunological synapse and the actin cytoskeleton: molecular hardware for T cell signaling. Nat Immunol 2000;1:23–9. [PubMed: 10881170]
39. Leekumjorn S, Wu Y, Sum AK, Chan C. Experimental and computational studies investigating trehalose protection of HepG2 cells from palmitate induced toxicity. Biophys J 2008;94:2869–83.10.1529/biophysi.107.120717 [PubMed: 18096630]
40. Unger RH, Orci L. Lipotoxic diseases of nonadipose tissues in obesity. Int J Obes Relat Metab Disord 2000;24 (Suppl 4):S28–32. [PubMed: 11126236]
41. Kook S, Hoon Kim D, Ryeol Shim S, Kim W, Chun J, Song WK. Caspase-dependent cleavage of tensin induces disruption of actin cytoskeleton during apoptosis. Biochem Biophys Res Commun 2003;303:37–45. [PubMed: 12646163]
42. Sanderson P, MacPherson GG, Jenkins CH, Calder PC. Dietary fish oil diminishes the antigen presentation activity of rat dendritic cells. J Leukoc Biol 1997;62:771–7. [PubMed: 9400818]
43. Zeyda M, Saemann MD, Stuhlmeier KM, et al. Polyunsaturated fatty acids block dendritic cell activation and function independently of NF-κB activation. J Biol Chem 2005;280:14293–301. [PubMed: 15684433]
44. Khair-el-Din TA, Sicher SC, Vazquez MA, Wright WJ, Lu CY. Docosahexaenoic acid, a major constituent of fetal serum and fish oil diets, inhibits IFN gamma-induced ia-expression by murine macrophages in vitro. J Immunol 1995;154:1296–306. [PubMed: 7822798]
45. Hughes DA, Pinder AC. n-3 polyunsaturated fatty acids inhibit the antigen-presenting function of human monocytes. Am J Clin Nutr 2000;71:357S–60. [PubMed: 10617997]
46. Hughes DA, Pinder AC, Piper Z, Johnson IT, Lund EK. Fish oil supplementation inhibits the expression of major histocompatibility complex class II molecules and adhesion molecules on human monocytes. Am J Clin Nutr 1996;63:267–72. [PubMed: 8561070]

47. Geyeregger R, Zeyda M, Zlabinger GJ, Waldhausl W, Stulnig TM. Polyunsaturated fatty acids interfere with formation of the immunological synapse. J Leukoc Biol 2005;77:680–8. [PubMed: 15703198]

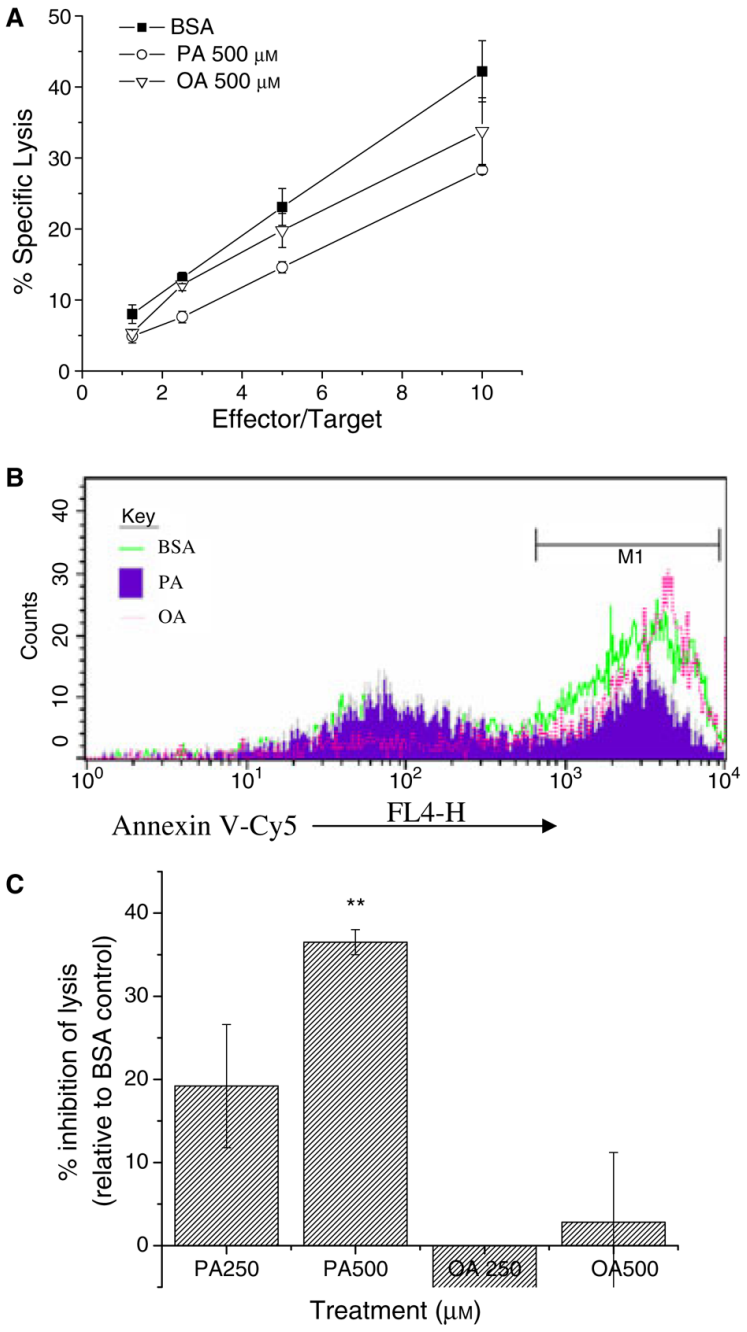

Figure 1.

PA-treated APC are resistant to lysis by activated CTL. (A) Representative experiment comparing specific lysis of APC as a function of effector to lipid-treated targets. Target T2-K^b cells were incubated with 250–500 μM PA or OA complexed to BSA, or BSA alone, for 12 h at 37 °C, peptide pulsed, labelled with ^{51}Cr and mixed with activated 2C CTL for 4 h. ^{51}Cr release was measured in terms of radioactive counts in the supernatants normalized to maximal release and corrected for leakage, as described in the Materials and methods. (B) Sample histogram of CTL lysis measured by Annexin V-Cy5 staining using flow cytometry. Control or lipid-treated T2-K^b-YFPs were incubated with activated CTL for 2 h, at which time apoptotic cells were identified as YFP^+ Annexin V-$Cy5^+$7-AAD^-. (C) Average change in

percent specific lysis at E/T = 5/1. Data in C (average ± SE) are from five independent measurements (**$P < 0.01$).

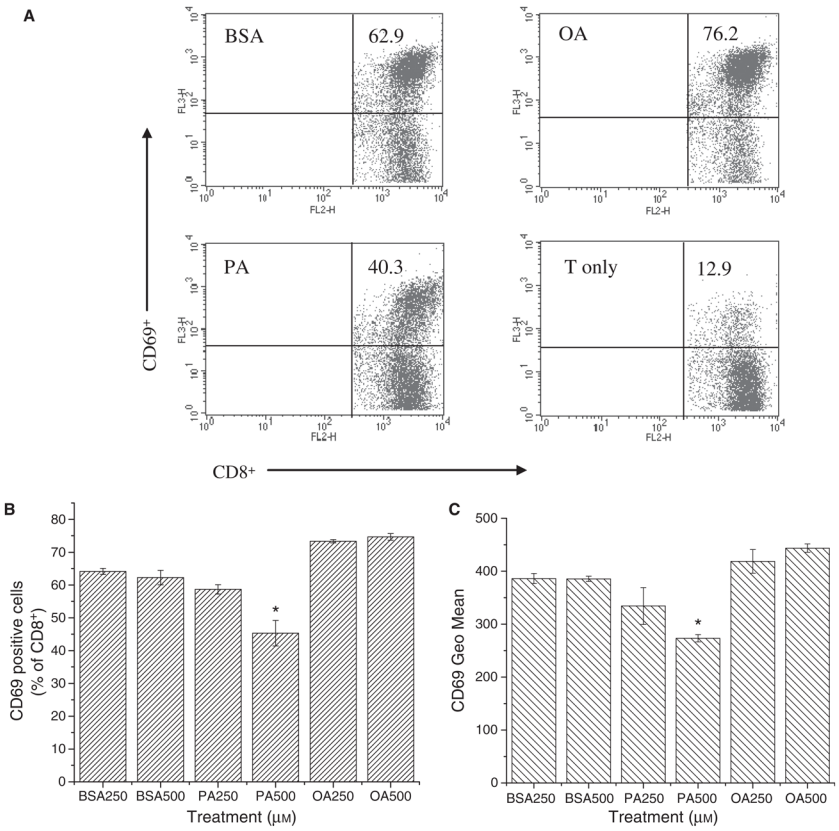

Figure 2.

PA-treatment of APC inhibits their ability to activate naïve T cells. (A) Sample flow cytometry fluorescence dot plots of naïve T-cell activation, assessed by staining with anti-mouse CD69-PECy7 and CD8-PE. Cells are gated on live $CD8^+$ T cells. The numbers in the upper right quadrant are the percentage of $CD69^+$ T cells activated with T2-K^b cells treated with 500 μM BSA, PA, or OA. T cell only is the negative control. (B) Change in percentage of activated $CD69^+$ T cells with and without lipid treatment. (C) Geometric mean of CD69 surface expression of $CD8^+$ T cells stimulated with BSA-, PA-, or OA-treated T2-K^bs. T2-K^b cells were treated with 250–500 μM PA or OA for 12 h at 37 °C, peptide pulsed, and then mixed with naïve T cells isolated from the spleens of 2C transgenic mice at a ratio of 1/1. Activation of naïve T cells was measured with flow cytometry 6 h later. Data in B and C (average ± SE) are from three independent measurements (*$P < 0.01$).

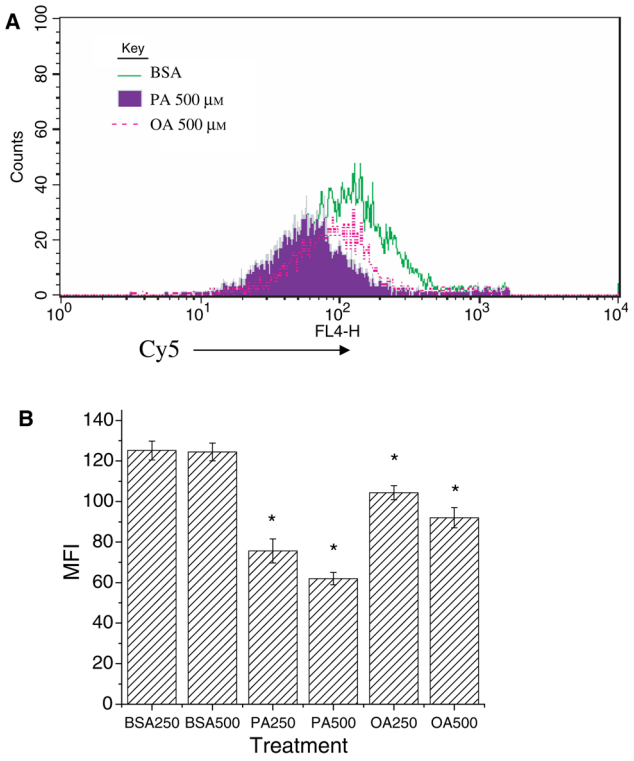

Figure 3.

Fatty acid treatment of APC lowers MHC class I surface expression. T2-K^b cells were treated for 12 h with 250–500 μM BSA, PA, or OA at 37 °C and pulsed with 1 nM SIY. MHC class I surface expression was measured with antibody binding (20.8.4s) using flow cytometry. (A) Sample flow cytometry histogram of 20.8.5-Cy5 staining for MHC class I. (B) Median fluorescence intensity (MFI) values (average ± SE) of 20.8.5-Cy5 staining for MHC class I on T2-K^b cells treated with BSA, PA or OA from three independent measurements (*$P < 0.05$).

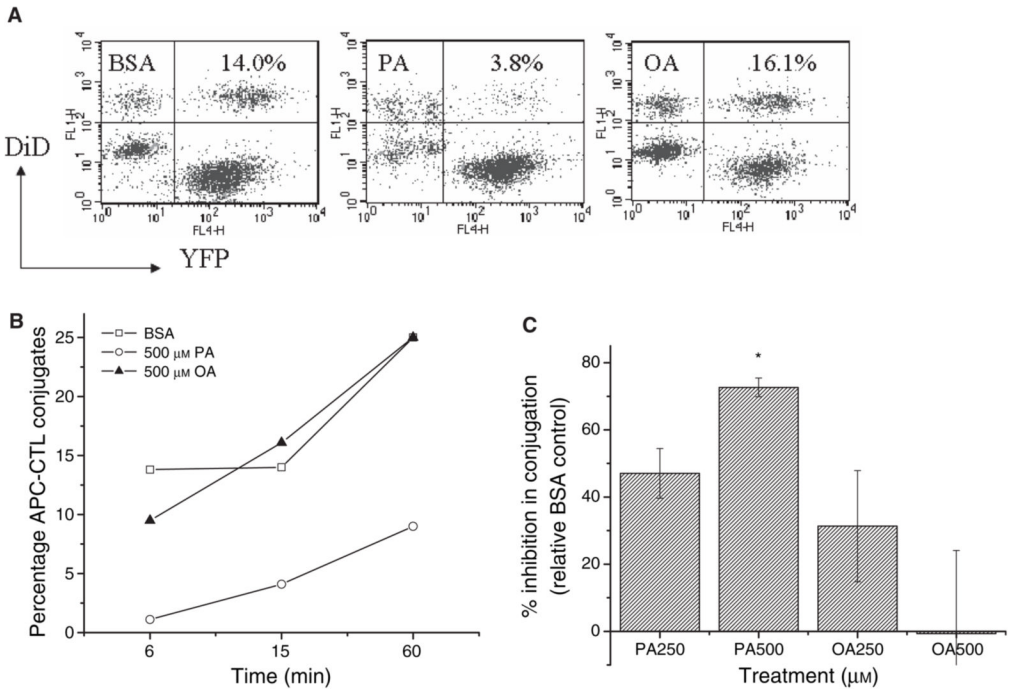

Figure 4.

PA-treatment of APC inhibits conjugation with activated CTL. (A) Sample flow cytometry dot plots of activated CTL, T2-K^b-YFPs, and conjugates. T2-K^b-YFP cells were treated with BSA, PA, or OA for 12 h, peptide pulsed, and mixed with DiD loaded CTL at a ratio of 1/1. Conjugates were identified as YFP^+DiD^+ after 15 min of incubation at 37 °C. The numbers in the upper right quadrant are the percentage of T cells conjugated. (B) Change in the rate of APC–T-cell conjugation (percentage of T cells conjugated to APC). Data are pooled from two separate experiments. (C) Change in APC–T-cell conjugation (average ± SE) relative to the BSA control from three to four independent measurements at 15 min (*$P < 0.01$).

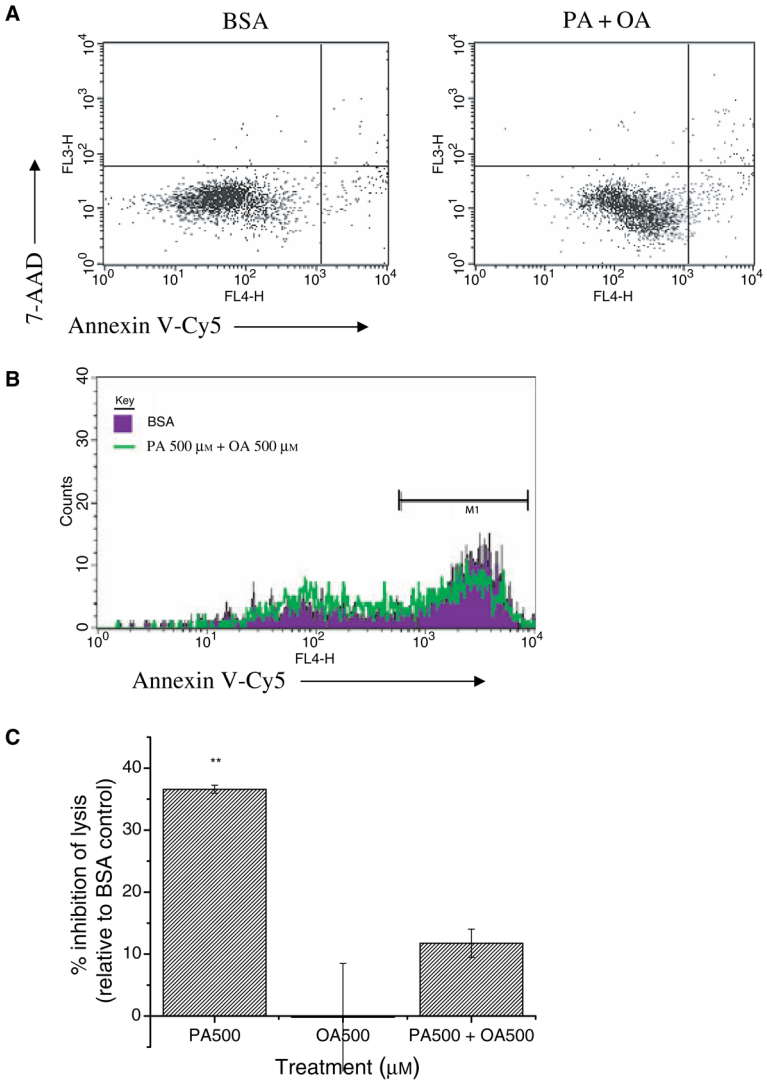

Figure 5.

OA-treatment of APC prevents the effects of PA on antigen presentation. (A) Treatment of T2-K^bs with 500 μM PA + 500 μM OA does not affect cell viability. Sample flow cytometry dot plots of Annexin V-Cy5, 7-AAD staining. Cells are greater than 90% viabile (lower left quadrant). (B) CTL lysis of T2-K^b-YFP cells treated with BSA or 500 μM PA + 500 μM OA. Cells were treated for 12 h at 37 °C, peptide pulsed, and mixed with activated CTL (E/T = 5) for 2 h at which time apoptotic cells were identified as YFP^+ Annexin $V\text{-}Cy5^+$ $7AAD^-$. (C) Change (average ± SE) in lysis is from two to three independent measurements (**$P < 0.01$).

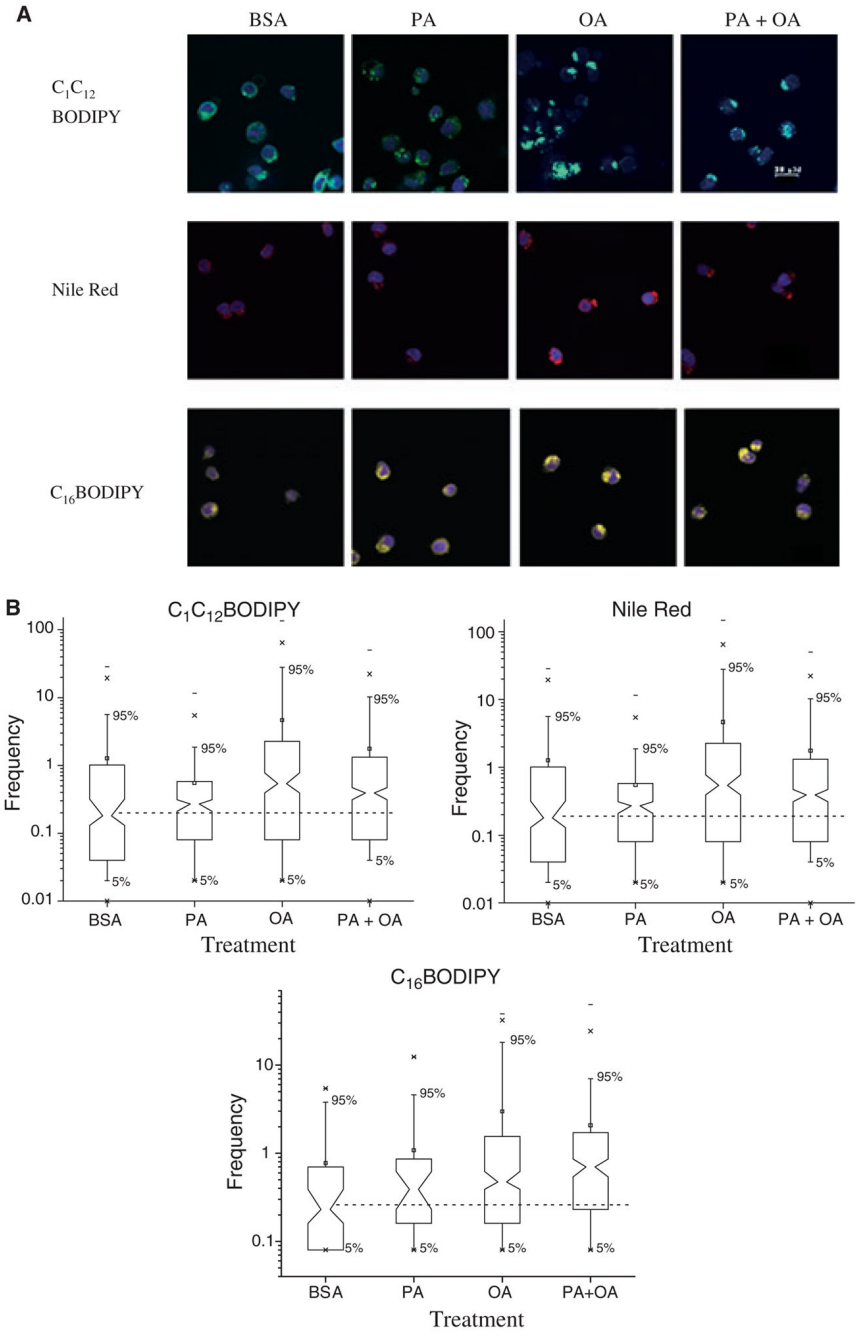

Figure 6.

Accumulation of fatty acids into triglyceride-rich lipid droplets protects against changes in antigen presentation. (A) Confocal fluorescence microscopy images of C_1C_{12} BODIPY (green), Nile Red (red), or C_{16}BODIPY (yellow) in T2-K^b cells treated for 12 h with BSA, 500 μM PA, 500 μM OA, or 500 μM PA + 500 μM OA. Images are false coloured and the nucleus is stained with DAPI (blue). C_1C_{12}BODIPY and Nile Red report on accumulation of monounsaturated fatty acids in neutral lipid stores and C_{16}BODIPY reports on incorporation of palmitate. (B) Box plot statistics for the fluorscence microscopy data represented in A for n = 31–43 cells per treatment condition. The frequency is area (pixels^2) occupied by C_1C_{12}BODIPY, Nile red, or C_{16}BODIPY in lipid droplets of T2-K^b cells above a defined

threshold. Note that non-overlapping notches (dashed line) represent statistical significance [27].

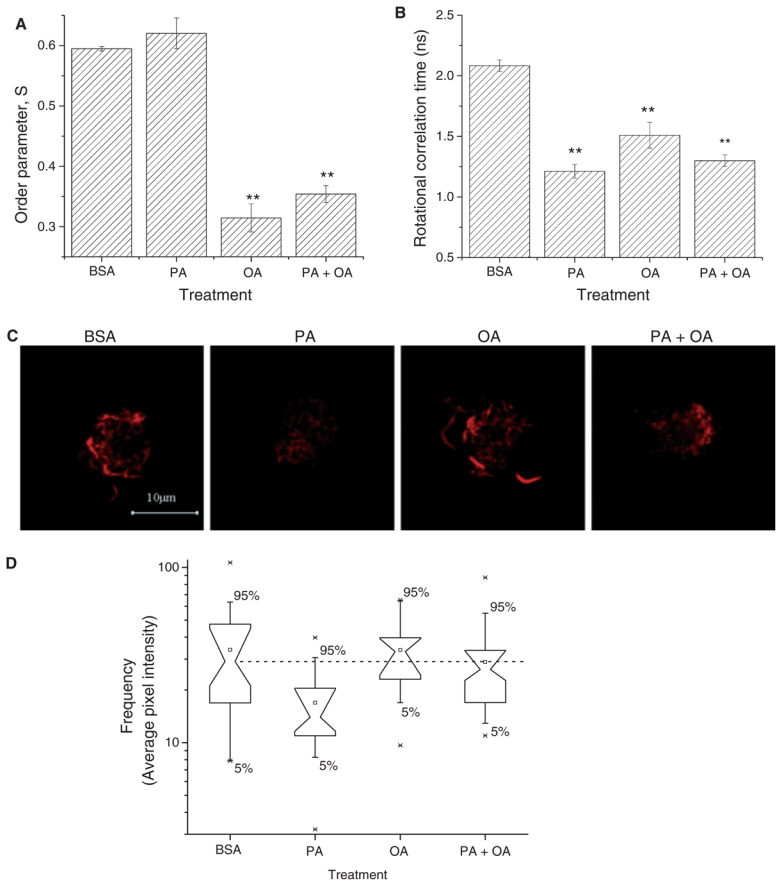

Figure 7.

PA and OA exert differential effects on the structure of the plasma membrane. (A) The effects of PA- and OA-treatment on plasma membrane structure were assessed using time-resolved fluorescence anisotropy measurements. Data were analysed using an empirical sum-of-three exponentials model, which quantifies probe order in terms of (A) the order parameter, S, and probe rotational dynamics in terms of (B) the average rotational correlation time. (C) Changes in actin remodeling of the plasma membrane was assessed with phalloidin (red) binding on APC using confocal fluorescence microscopy. (D) Box plot statistics for the fluorescence microscopy data represented in C for n = 25–30 cells per condition. The frequency is pixel intensity of phalloidin after subtraction of background. Note that non-overlapping notches (dashed line) of the box plots represents statistical significance [27]. T2-K^b cells were treated for 12 h with BSA, 500 μM PA, 500 μM OA, or 500 μM PA + 500 μM OA. Values in A–B are average ± SE from two independent experiments (*P < 0.05, **P < 0.01, P < 0.001).

Table 1

Time-resolved lifetimes and fluorescence anisotropy data analysed with the BRD model.

Treatment	D_{perp} (ns^{-1})	F_{random}	Intensity-weighted average lifetime (ns)
BSA (control)	0.142 ± 0.024	0.392 ± 0.020	8.840 ± 0.312
PA	0.222 ± 0.016**	0.378 ± 0.024	8.727 ± 0.087
OA	0.210 ± 0.028**	0.608 ± 0.037**	7.464 ± 0.136*
PA + OA	0.205 ± 0.023*	0.605 ± 0.003**	7.980 ± 0.175

FFA, free fatty acids; PA, palmitic acid; OA, oleic acid.

*$P < 0.05$,

**$P < 0.01$.

T2-K^b cells were treated for 12 h at 37 °C with BSA alone, or with FFA/BSA complexes consisting of 500 μM PA, 500 μM OA, or 500 μM PA + 500 μM OA and loaded with DPH at a lipid to probe ratio of 300:1. The BRD model quanitifes probe dynamics in terms of the diffusion coefficient for DPH rotation about its long axis, D_{perp}, and probe orientational order in terms of the the disorder parameter, F_{random}, which is proportional to the overlap of the orientaional probability distribution with randomly oriented DPH [26].